

## Influence of the Morphology of Electrodeposited Nanoparticles on the Activity of Organic Halide Reduction

Bart Geboes<sup>a,b</sup>, Bart Vanrenterghem<sup>a</sup>, Jon Ustarroz<sup>b</sup>, Danny Pauwels<sup>a</sup>, Sotiris Sotiropoulos<sup>c</sup>, Annick Hubin<sup>b</sup> and Tom Breugelmans<sup>a,b,\*</sup>

<sup>a</sup> University of Antwerp, Research Group Advanced Reactor Technology, Salesianenlaan 90, 2660 Hoboken, Belgium

<sup>b</sup> Vrije Universiteit Brussel, Research Group Electrochemical and Surface Engineering, Pleinlaan 2, 1050 Brussels, Belgium

<sup>c</sup> Aristotle University of Thessaloniki, Department of Chemistry, University Campus, Thessaloniki 54124, Greece  
 tom.breugelmans@uantwerpen.be

Silver nanoparticles (NP) were deposited on glassy carbon substrates using a potentiostatic dual pulse method in acetonitrile containing 1 mM AgNO<sub>3</sub> + 0.1 M LiClO<sub>4</sub>. The high amount of control on the NP synthesis was utilized to investigate the influence of the NP morphology on the catalytic activity of an organic electrosynthesis reaction. Nucleation pulses at -0.4, -0.6 and -0.8 V vs. Ag/AgCl were applied in chronoamperometry measurements. Scanning electron microscopy (SEM) indicated a significant dependency of NP morphology on nucleation potential. Nucleation pulses at lower overpotential resulted in an average particle size of 116 nm, while higher overpotentials produced NP's with sizes as low as 76 nm. For the organic electrosynthetic halide reduction, benzyl bromide was used as a model molecule. The benzyl bromide reduction activity was determined using cyclic voltammetry (CV). A proportional correlation between the nucleation peak potential and benzyl bromide reduction activity was observed. Peak potentials of the prepared NP's with nucleation pulses of high overpotential (-0.8 V) revealed even a positive shift of 83 mV compared to a bulk Ag disk electrode. There was no indication of an altered reaction mechanism since the benzyl bromide reduction wave was characterized as a process of diffusive nature and calculated apparent transfer coefficients ( $\alpha'$ ) of the NP electrodes varied around 0.3. This is an indication of a concerted reaction mechanism in compliance with the mechanism reported on bulk Ag.

### 1. Introduction

In recent years there has been a growing search for clean, catalytic and environmentally friendly methodologies in organic synthesis. To tackle these issues, an electrosynthetic methodology can be applied. Electrochemical syntheses mostly need fewer steps, produce less waste, provide a cheaper reagent and require less auxiliaries. (Schäfer 2011) Electrochemical C-C bond formation through reactive intermediates can result in a wide range of interesting chemicals. However, a major drawback is that those electrosynthetic processes require very negative electrode potentials that are inadequate for use in industrial production processes due to exuberant energy costs. Attempts to reduce the large overpotentials are directed towards improving catalytic activity of the electrode materials. (Bellomunno et al. 2005; Jouikov & Simonet 2010)

One of the most investigated electrosynthesis reactions in recent years has been the organic halide reduction, both application (Zhang et al. 2010) and mechanistic (Isse et al. 2008) studies were performed. Electrochemical reduction of organic halides has important applications in the reduction of environmental pollutants, carbon fixation and upgrading of organics through C-C bond formation. (Niu et al. 2008; Durante et al. 2012) Besides transition metal complexes (Duñach et al. 2003) several catalytic surfaces haven been studied for the direct one-electron reduction of organic halides. Ag, Cu, Au, Pd and Pb have shown significantly increased reduction activities. Compared to an inert glassy carbon electrode Ag shows the highest activity increase. This is due to a strong involvement of the cathode surface in the reaction

intermediates. (Isse et al. 2009) Potential shifts of up to 500 mV have been reported. (Isse et al. 2008) Despite this relatively large shift, the reduction potentials for C-X activation in benzyl chloride remain in the vicinity of -1.75 V relative to the saturated calomel electrode (SCE).

Attempts to further reduce the large overpotential in C-X activation have been directed towards improving catalytic activity by (a) changing from bulk electrodes to nanoparticles (NP) dispersed on a support and (b) by introducing a second metal. Nanoscale materials show unique properties different from the bulk material due to their reduced dimensions (1-100nm). These properties can be tuned by changing morphological characteristics such as size and shape. (Burda et al. 2005) In the context of electrocatalysis nanoparticles can enhance mass transport and electrocatalytic activity, besides offering an increased active surface area. A variety of electrochemical approaches (potentiostatic, galvanostatic and potentiodynamic) have been utilised to synthesize those supported nanoparticles. The common aim here is to control synthesis parameters to obtain NP distributions with low size and shape dispersions. Therefore a potentiostatic double pulse technique was developed by the groups of Penner and Plieth to avoid size dispersion as a result of progressive nucleation and diffusion coupling. (Sandmann et al. 2000; Liu et al. 2001) Some authors have used NP electrodeposits as organic halide reduction electrocatalysts. (Zhang et al. 2010; Perini et al. 2014) However no catalytic improvement of single metal NP's over the bulk metal has been reported yet for benzyl bromide reduction.

In this work benzyl bromide is used as a model molecule to study the organic halide reduction. The link between the morphology of the catalyst material and the electrocatalytic activity is investigated. Therefore silver nanoparticles (NP) are electrochemically deposited on a glassy carbon substrate with a high amount of control on their size and distribution using a dual pulse potentiostatic procedure.

## 2. Experimental

### 2.1 Formation of silver nanoparticles through electrodeposition

The silver nanoparticles were deposited on polished glassy carbon planar electrodes. The polishing procedure consisted out of sequential polishing with 1  $\mu\text{m}$ , 0.3  $\mu\text{m}$  and 0.05  $\mu\text{m}$  alumina powders (Struers). After polishing the electrodes were rinsed with ultra-pure water (18.2 M $\Omega$  cm) and isopropanol respectively under sonication. The silver planar electrode, used as a benchmark, was polished in an identical way prior to all experiments. The electrodeposition was carried out in a three-electrode cell with the planar glassy carbon electrode as working electrode, a platinum sheet as counter electrode and a saturated Ag/AgCl reference electrode. The electrolyte solution consisted of 0.1 M LiClO<sub>4</sub> (Acros, p.a.) in acetonitrile (BioSolve, HPLC grade) thermostated at 25 °C. The reference electrode was separated by the working electrode through a salt bridge, preventing chloride or water contamination in the measurement medium. Silver ions were provided in the form of AgNO<sub>3</sub> (99.9 %, Sigma Aldrich). All products were used as received. The electrodeposition was performed during chronoamperometry using a Autolab potentiostat/galvanostat PGSTAT 302F. A dual potential pulse technique was used. (Ustarroz et al. 2011) A short nucleation pulse at high overpotential and a longer growth pulse at low overpotential were carried out.

### 2.2 Surface and electrochemical characterization of deposited nanoparticles

The activity of the deposited electrodes towards benzyl bromide reduction was assessed using cyclic voltammetry (CV). A conventional three-electrode cell was used with the prepared electrodes as working electrode. The same counter and reference electrodes were used as with the deposition measurements. An acetonitrile based electrolyte solution was used with 0.1 M tetrabutylammonium perchlorate (Bu<sub>4</sub>NClO<sub>4</sub>) (Acros, 99%+ ) thermostated at 25 °C and saturated with nitrogen to avoid the influence of dissolved oxygen. The CV measurements were carried out using the Autolab PGSTAT 302F potentiostat

The surface morphology of the deposited nanoparticles was characterized using a Jeol JSM 7000 field emission scanning electron microscope (FESEM). Beam intensities of 15keV were used. After the deposition procedure the GC disk electrodes containing silver NP's were rinsed in acetonitrile and dried to the air prior to the SEM measurements.

## 3. Results and discussion

### 3.1 Dual pulse electrodeposition of silver nanoparticles

Cyclic voltammograms were recorded at 50mV/s in a acetonitrile solution containing 0.1 M LiClO<sub>4</sub> + 1mM AgNO<sub>3</sub> on a bare glassy carbon electrode. These measurements were recorded prior to the dual pulse deposition procedure to estimate possible values of the nucleation potential ( $E_n$ ) and growth potential ( $E_g$ ).

Figure 1 shows the resulting first and second scan displaying the characteristic features of diffusion-controlled electrodeposition and stripping. The onset potential of the reduction peak in the second scan (102 mV) is shifted towards more positive values compared to scan 1 (-18 mV). This indicates that the energy threshold for Ag deposition on glassy carbon is higher compared to Ag substrates. The onset of -18 mV in scan 1 determines the critical deposition potential ( $E_{crit}$ ). The nucleation overpotential ( $\eta_n$ ) is defined as the difference between the onset potentials of the first and second scan and amounts to 120 mV.

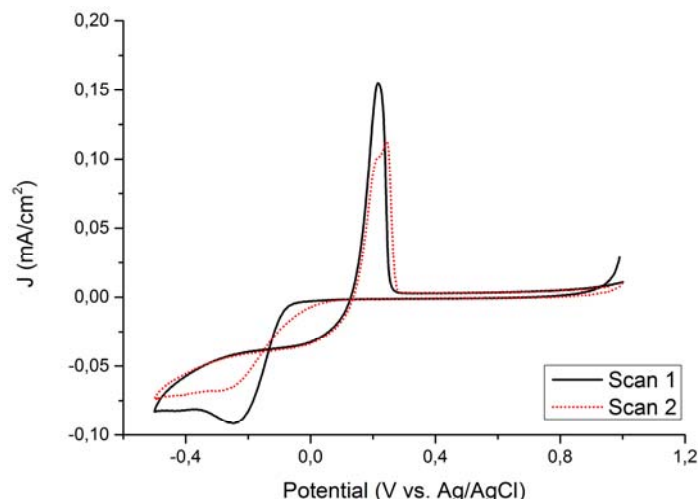


Figure 1: Cyclic voltammogram at  $50 \text{ mV s}^{-1}$  of  $1 \text{ mM AgNO}_3$  in acetonitrile +  $0.1 \text{ M LiClO}_4$  at glassy carbon electrodes ( $0.6 \text{ mm}$  diameter). The first two scans are shown, indicating the deposition overpotential.

Solvent, supporting electrolyte and  $\text{Ag}^+$  concentration all influence the morphology of deposited NP's. In the potentiostatic dual pulse technique four additional deposition parameters can be used to control NP morphology: nucleation potential ( $E_n$ ), nucleation time ( $t_n$ ), growth potential ( $E_g$ ) and growth time ( $t_g$ ). Depositions were performed with different nucleation parameters while  $E_g$  was kept constant at  $-0.12 \text{ V}$  and growth times of 100s were maintained. The growth kinetics of Ag particles in aqueous solutions are extremely high and give smaller margins for controlling particle morphology. The use of acetonitrile as solvent overcomes this problem as can be concluded from the peak width  $|E_p - E_{p/2}|$  of the reduction waves in the potential region of  $0 \text{ V}$  to  $-0.4 \text{ V}$  in Figure 1 (105 mV and 160 mV respectively). Especially in scan 2 which is important for the growth pulse, the peak width is relatively broad. The growth pulse is ideally chosen more positive to the critical deposition potential and more negative compared to the reversible potential. Since only small current densities are formed in this potential region a more negative growth potential of  $-0.12 \text{ V}$  is utilized.

Table 1: Voltammetric parameters for the reduction of  $1 \text{ mM}$  benzyl bromide in acetonitrile +  $0.1 \text{ M Bu}_4\text{NClO}_4$  obtained with a scan rate of  $50 \text{ mV/s}$ .

	$E_n$ (V vs. Ag/AgCl)	$t_n$ (s)	$E_g$ (V vs. Ag/AgCl)	$T_g$ (s)	$E_p$ (V vs. Ag/AgCl)	$E_{p/2}$ (V vs. Ag/AgCl)	$\alpha'$
NP 1	-0.6	1	-0.12	100	-1.115	0.11	0.45
NP 2	-0.8	1	-0.12	100	-0.964	0.16	0.31
NP 3	-0.8	2	-0.12	100	-0.977	0.18	0.26
NP 4	-0.8	1.5	-0.12	100	-0.977	0.17	0.29
NP 5	-0.4	2	-0.12	100	-1.191	0.10	0.48

The deposition parameters and calculated voltammetric data of all prepared nanoparticle electrodes are summarized in Table 1. The electrodes are later referred to with their short names from the first column. The apparent transfer coefficient  $\alpha$  is calculated from the peak potential ( $E_p$ ) and half-wave potential ( $E_{p/2}$ ). SEM micrographs of two glassy carbon electrodes after the deposition procedure are shown in Figure 2. Nucleation potentials of  $-0.8 \text{ V}$  (a) and  $-0.4 \text{ V}$  (b) are used. The nucleation pulse at higher overpotential results in an average NP size of 76nm. Besides some coagulations that are formed, the deposited particles in electrode NP3 have a good dispersion. A dual particle size dispersion is observed in the micrograph of NP5, synthesized using a nucleation potential of only  $-0.4 \text{ V}$ .

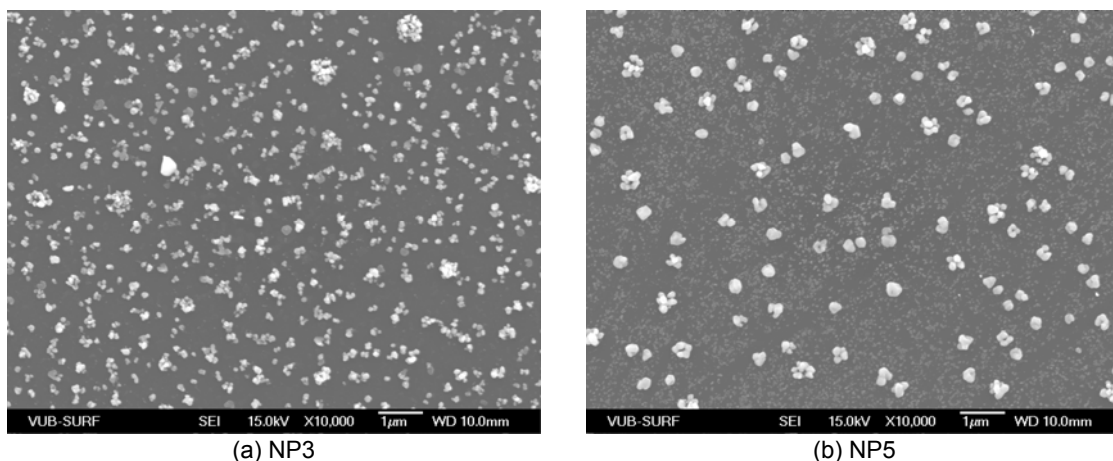


Figure 2: SEM micrographs of the glassy carbon substrate after Ag nanoparticle deposition with nucleation potentials ( $E_n$ ) of  $-0.8$  V (a) and  $-0.4$  V (b). Other deposition parameters are kept constant: nucleation time ( $t_n$ ) = 2 s; growth potential ( $E_g$ ) =  $-0.12$  V and growth time ( $t_g$ ) = 100 s.

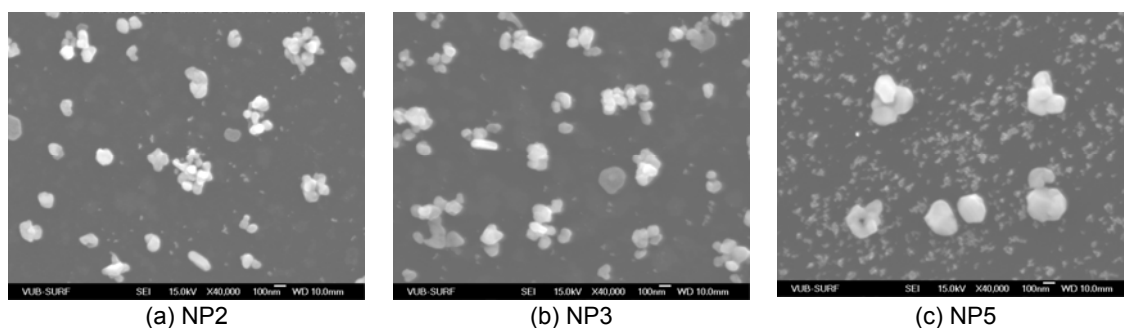


Figure 3: SEM micrographs of the glassy carbon substrate after Ag deposition with varying nucleation potentials and nucleation times. (a)  $E_n = -0.8$  V,  $t_n = 1$  s; (b)  $E_n = -0.8$  V,  $t_n = 2$  s and (c)  $E_n = -0.4$  V,  $t_n = 2$  s.

The larger particles in this deposition have a mean size of 116 nm and are significantly larger compared to NP3. SEM pictures at higher magnification (X 40,000) are shown for electrodes NP2, NP3 and NP5 in Figure 3. The nucleation potential in deposition NP2 and NP3 is  $-0.8$  V. The average particle size in NP2 is 78 nm and comparable to NP3. However, the particle density of 811 particles/ $100 \mu\text{m}^2$  in NP3 is significantly higher compared to 501 particles/ $100 \mu\text{m}^2$  in NP2. The longer nucleation pulse of 2 s compared to 1 s is probably the cause for this. Using the higher magnification it is even more clear that a large size dispersion is formed in NP5 (Figure 3 c). Besides the larger particles with a mean size of 116 nm much smaller particles can be observed only several nm in size. The total count of the larger circular sized particles is only 174 particles/ $100 \mu\text{m}^2$ . The different  $E_n$  appears to have a large influence on the morphology.

### 3.2 Benzyl bromide reduction activity

The electrochemical activity of all deposited nanoparticles is tested for the benzyl bromide reduction. Cyclic voltammetry is used as fast and accurate measure for catalytic activity. The potential value of the single reduction wave observed for organic halide reductions indicates the strength of the catalytic effect.

In Figure 4 the reduction wave for a bare glassy carbon electrode (full black line) is shown as a reference for a non-catalytic substrate. The corresponding peak potential is  $-1.68$  V vs. Ag/AgCl. The planar Ag electrode in Figure 4 shows a sharp reduction peak (dashed blue line) at a much lower overpotential ( $-1.06$  V) and is indicative for its high catalytic activity towards C-X bond cleavage. Also in Figure 4 cyclic voltammograms for NP modified electrodes are shown with  $E_n = -0.4$  V (NP5),  $E_n = -0.6$  V (NP1) and  $E_n = -0.8$  V (NP3). Electrode NP5 has a 131 mV lower reduction potential compared to bulk Ag. This lower catalytic activity despite the presence of small particles in the nm range (see Figure 3 c) indicates no particle size effect is at play. The higher nucleation potential used in NP1 does not result in a dual particle size dispersion and further increases the benzyl bromide reduction potential to 55 mV below bulk Ag. The incremental effect of the higher nucleation potential even amounts to an increase in reduction potential of 83 mV for NP 3 compared to bulk Ag.

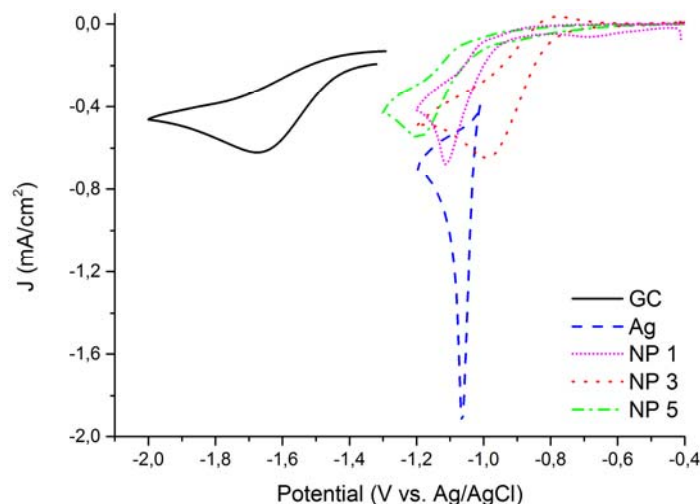


Figure 4: Cyclic voltammetry of 1 mM benzyl bromide in  $CH_3CN + 0.1 M Bu_4NClO_4$  at  $v = 50 mV/s$ . CV curves obtained at bulk electrodes (GC and Ag) and NP deposited electrodes.

The lower reduction peak densities for all NP electrodes is probably due to an overestimation of the active surface area. Current densities here are determined in respect to the geometric surface area of the electrode which is not fully covered with nanoparticles. NP coverage determined with SEM ranges between 7 % and 15 % in all measured depositions. However SEM only measures the projected particle area thus these values cannot be used as a correction factor for active surface area.

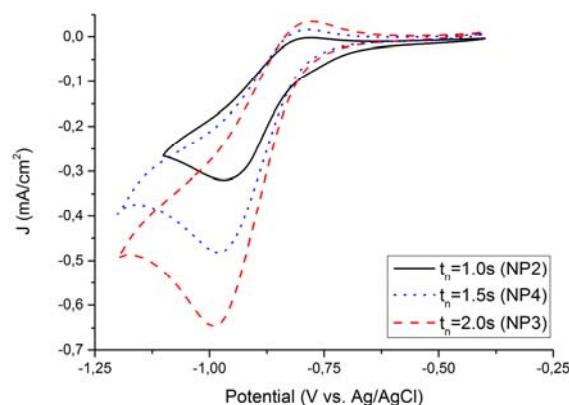


Figure 5: Cyclic voltammetry of 1 mM benzyl bromide in  $CH_3CN + 0.1 M Bu_4NClO_4$  at  $v = 50 mV/s$ . CV curves obtained at NP depositions using different nucleation times.

The influence of nucleation time ( $t_n$ ) on catalytic activity is visualized in Figure 5. Three depositions with identical nucleation potential (-0.8 V) and growth parameters are shown. Reduction potentials are very similar for the three electrodes (see Table 1). Particle size and shape are determined by  $E_n$  thus similar catalytic activity between these depositions is to be expected. The apparent increase in reduction peak current density with nucleation time clearly stands out from Figure 5. The higher peak current density of NP3 ( $-0.65 mA/cm^2$ ) compared to NP2 ( $-0.32 mA/cm^2$ ) could be the result of the higher particle density measured earlier using SEM analysis. A higher particle density results in a larger electrochemical active surface area and thus higher peak current. The increase in peak current density of NP3 in respect to NP2 is in the same order of magnitude as their respective particle coverage of 811 particles/ $100 \mu m^2$  and 501 particles/ $100 \mu m^2$  respectively.

To exclude the possibility that the shift in reduction potential of NP3 relative to the planar Ag electrode of 83 mV is due to an altered reaction mechanism two indications are investigated. First the benzyl bromide reduction wave is measured at multiple scan rates between 50 mV/s and 1 V/s. A good correlation ( $R^2 = 0.9913$  -not shown) is found between peak potential and the square root of the scan rate. The benzyl bromide reduction is thus characterized as a process of diffusive nature (Falciola et al. 2006). Second the apparent transfer coefficient ( $\alpha'$ ) of the NP3 electrode was found to be 0.26. This is an indication of a concerted reaction mechanism in compliance with the mechanism reported on bulk Ag.

#### 4. Conclusions

Silver nanoparticles have been deposited on glassy carbon substrates using a potentiostatic dual pulse method in acetonitrile containing 1 mM AgNO<sub>3</sub> + 0.1 M LiClO<sub>4</sub>. The nature of the nanoclusters was tuned by changing nucleation parameters. Longer nucleation pulses increased particle coverage and resulted in proportionally higher benzyl bromide reduction current densities. Nucleation pulses at low overpotential (-0.4 V), applied during chronoamperometry resulted in average particle sizes of 116 nm. High overpotential pulses of -0.8 V produced NP's with sizes as low as 76 nm. A proportional correlation between nucleation pulse overpotential and benzyl bromide reduction activity was determined. Peak potentials of the prepared NP's with nucleation pulses of high overpotential (-0.8 V) revealed even a positive shift of 83 mV compared to a bulk Ag disk electrode. There appeared to be no indication of an altered reaction mechanism since the benzyl bromide reduction wave was characterized as a process of diffusive nature and the calculated apparent transfer coefficients ( $\alpha'$ ) of the NP electrodes varied around 0.3. This is an indication of a concerted reaction mechanism in compliance with the mechanism reported on bulk Ag.

#### References

- Bellomunno, C., Bonanomi, D., Falciola, L., Longhi, M., Mussini, P.R., Doubova, L.M. & Di Silvestro, G., 2005. Building up an electrocatalytic activity scale of cathode materials for organic halide reductions. *Electrochimica Acta*, 50(11), pp.2331–2341.
- Burda, C., Chen, X., Narayanan, R. & El-Sayed, M. a, 2005. Chemistry and properties of nanocrystals of different shapes. *Chemical reviews*, 105(4), pp.1025–102.
- Duñach, E., Franco, D. & Olivero, S., 2003. Carbon–Carbon Bond Formation with Electrogenenerated Nickel and Palladium Complexes. *European Journal of Organic Chemistry*, 2003(9), pp.1605–1622.
- Durante, C., Huang, B., Isse, A.A. & Gennaro, A., 2012. Electrocatalytic dechlorination of volatile organic compounds at copper cathode. Part II: Polychloroethanes. *Applied Catalysis B: Environmental*, 126, pp.355–362.
- Falciola, L., Gennaro, A., Isse, A.A., Mussini, P.R. & Rossi, M., 2006. The solvent effect in the electrocatalytic reduction of organic bromides on silver. *Journal of Electroanalytical Chemistry*, 593(1-2), pp.47–56.
- Isse, A. a, Gottardello, S., Durante, C. & Gennaro, A., 2008. Dissociative electron transfer to organic chlorides: electrocatalysis at metal cathodes. *Physical chemistry chemical physics: PCCP*, 10(17), pp.2409–16.
- Isse, A.A., Berzi, G., Falciola, L., Rossi, M., Mussini, P.R. & Gennaro, A., 2009. Electrocatalysis and electron transfer mechanisms in the reduction of organic halides at Ag. *Journal of Applied Electrochemistry*, 39(11), pp.2217–2225.
- Jouikov, V. & Simonet, J., 2010. The one-electron cleavage of benzylic bromides at palladium and palladized cathodes: Benzyl radicals generation and immobilization onto solid interfaces. *Electrochemistry Communications*, 12(3), pp.331–334.
- Liu, H., Favier, F., Ng, K., Zach, M. & Penner, R., 2001. Size-selective electrodeposition of meso-scale metal particles: a general method. *Electrochimica Acta*, 47(5), pp.671–677.
- Niu, D.-F., Xiao, L.-P., Zhang, A.-J., Zhang, G.-R., Tan, Q.-Y. & Lu, J.-X., 2008. Electrocatalytic carboxylation of aliphatic halides at silver cathode in acetonitrile. *Tetrahedron*, 64(46), pp.10517–10520.
- Perini, L., Durante, C., Favaro, M., Agnoli, S., Granozzi, G. & Gennaro, A., 2014. Electrocatalysis at palladium nanoparticles: Effect of the support nitrogen doping on the catalytic activation of carbonhalogen bond. *Applied Catalysis B: Environmental*, 144, pp.300–307.
- Sandmann, G., Dietz, H. & Plieth, W., 2000. Preparation of silver nanoparticles on ITO surfaces by a double-pulse method. *Journal of Electroanalytical Chemistry*, 491(1-2), pp.78–86.
- Schäfer, H.J., 2011. Contributions of organic electrosynthesis to green chemistry. *Comptes Rendus Chimie*, 14(7-8), pp.745–765.
- Ustarroz, J., Hammons, J. a., Van Ingelgem, Y., Tzedaki, M., Hubin, A. & Terry, H., 2011. Multipulse electrodeposition of Ag nanoparticles on HOPG monitored by in-situ by Small-Angle X-ray Scattering. *Electrochemistry Communications*, 13(12), pp.1320–1323.
- Zhang, G.P., Kuang, Y.F., Liu, J.P., Cui, Y.Q., Chen, J.H. & Zhou, H.H., 2010. Fabrication of Ag/Au bimetallic nanoparticles by UPD-redox replacement: Application in the electrochemical reduction of benzyl chloride. *Electrochemistry Communications*, 12(9), pp.1233–1236.